

1 **Nuclease escape elements protect messenger RNA against cleavage by**
2 **multiple viral endonucleases**

3

4 Mandy Muller¹; Britt A. Glaunsinger^{1,2,3*}

5 ¹. Department of Plant and Microbial Biology, University of California, Berkeley, California,
6 USA CA 94720-3370

7 ². Department of Cell and Molecular Biology, University of California, Berkeley, California,
8 USA CA 94720-3370

9 ³. Howard Hughes Medical Institute

10

11 * Corresponding author; glaunsinger@berkeley.edu

12 **Short Title:** Viral nuclease escape elements

13 **ABSTRACT**

14 During lytic Kaposi's sarcoma-associated herpesvirus (KSHV) infection, the viral endonu-
15 clease SOX promotes widespread degradation of cytoplasmic messenger RNA (mRNA).
16 However, select mRNAs, including the transcript encoding interleukin-6 (IL-6), escape SOX-
17 induced cleavage. IL-6 escape is mediated through a 3' UTR RNA regulatory element that
18 overrides the SOX targeting mechanism. Here, we reveal that this protective RNA element
19 functions to broadly restrict cleavage by a range of homologous and non-homologous viral
20 endonucleases. However, it does not impede cleavage by cellular endonucleases. The IL-6
21 protective sequence may be representative of a larger class of nuclease escape elements, as
22 we identified a similar protective element in the GADD45B mRNA. The IL-6 and GADD45B-
23 derived elements display similarities in their sequence, putative structure, and several
24 associated RNA binding proteins. However, the overall composition of their
25 ribonucleoprotein complexes appears distinct, leading to differences in the breadth of
26 nucleases restricted. These findings highlight how RNA elements can selectively control
27 transcript abundance in the background of widespread virus-induced mRNA degradation.

28

29 **AUTHOR SUMMARY**

30 The ability of viruses to control the host gene expression environment is crucial to promote
31 viral infection. Many viruses express factors that reduce host gene expression through
32 widespread mRNA decay. However, some mRNAs escape this fate, like the transcript
33 encoding the immunoregulatory cytokine IL-6 during KSHV infection. IL-6 escape relies on
34 an RNA regulatory element located in its 3'UTR and involves the recruitment of a
35 protective protein complex. Here, we show that this escape extends beyond KSHV to a
36 variety of related and unrelated viral endonucleases. However, the IL-6 element does not
37 protect against cellular endonucleases, revealing for the first time a virus-specific nuclease
38 escape element. We identified a related escape element in the GADD45B mRNA, which
39 displays several similarities with the IL-6 element. However, these elements assemble a
40 largely distinct complex of proteins, leading to differences in the breadth of their protective
41 capacity. Collectively, these findings reveal how a putative new class of RNA elements
42 function to control RNA fate in the background of widespread mRNA degradation by viral
43 endonucleases.

44

45 INTRODUCTION

46 A number of viruses restrict host gene expression to reduce competition for resources
47 and dampen immune responses. This 'host shutoff' phenotype can be triggered through a
48 range of mechanisms that operate at nearly every stage of the gene expression cascade.
49 Viruses whose host shutoff strategies involve the induction of widespread mRNA decay
50 include the alpha and gammaherpesviruses, vaccinia virus (VACV), influenza A virus (IAV),
51 and SARS coronavirus (SCoV) [1-5] In each of the above cases, mRNA degradation is
52 induced *via* one or more internal endonucleolytic cleavages in the target mRNA or, in the
53 case of VACV, direct removal of the mRNA 5' cap [5-9]. This is invariably followed by
54 exonucleolytic degradation of the cleaved fragment(s) by components of the mammalian
55 RNA decay machinery such as Xrn1 [1,10,11].

56 The viral strategy contrasts with basal mRNA degradation in eukaryotes, which is a
57 tightly regulated process that initiates with gradual shortening of the poly(A) tail, followed
58 by removal of the 5' cap prior to exonucleolytic degradation of the transcript body [12].
59 Although eukaryotes encode endonucleases, they are generally restricted to a highly
60 specific set of targets. For example, mRNAs containing premature stop codons are cleaved
61 by the Smg6 endonuclease during the translation-linked quality control process of
62 nonsense mediated decay (NMD) [13]. No-go decay is another form of quality control
63 activated in cases of ribosome stalling, although the specific endonuclease that cleaves the
64 mRNA remains unknown [14,15]. The use of endonucleases during quality control enables
65 more rapid removal of aberrant mRNAs from the translation pool, as their inactivation is
66 not reliant on the prior rate limiting steps of deadenylation and decapping. In this regard,

67 virus-induced mRNA decay resembles the cellular quality control mechanisms, but with
68 significantly expanded scope.

69 One of the well-studied viral endonucleases is the SOX protein encoded by ORF37 of
70 Kaposi's sarcoma-associated herpesvirus (KSHV). During lytic KSHV replication, SOX is
71 expressed with delayed early kinetics and its nuclease activity significantly reduces
72 cytoplasmic mRNA levels [16]. SOX is conserved throughout the herpesvirus family, but
73 only gammaherpesviral SOX homologs display ribonuclease activity in cells [16-18].
74 Perhaps surprisingly, its activity is not restricted to host mRNAs, and studies with the SOX
75 homolog from murine gammaherpesvirus 68 (MHV68) indicate that SOX activity helps fine
76 tune viral mRNA levels in a manner important for the *in vivo* viral lifecycle [19,20].
77 Although most mRNAs are subject to cleavage by SOX, a recent degradome-based
78 sequencing analysis together with studies on individual endogenous and reporter mRNAs
79 revealed that SOX cleavage sites are defined by a degenerate RNA motif [10,21]. The SOX-
80 targeting motif can be located anywhere within an mRNA and may be present multiple
81 times [10,21].

82 The observation that a targeting motif is present on SOX cleaved mRNAs suggests that
83 transcripts lacking this element should escape cleavage. Indeed, RNAseq analyses indicate
84 that approximately one-third of mRNAs are not depleted by SOX [22,23]. Studying these
85 'escapees' in aggregate is complicated, however, by the fact that multiple mechanisms can
86 promote apparent escape. These include lack of a targeting motif, indirect transcriptional
87 effects, and active evasion of cleavage [22,24-28]. This latter phenotype, termed dominant
88 escape, is particularly notable as it involves a specific RNA element whose presence in the
89 3' UTR of an mRNA protects against SOX cleavage, regardless of whether the RNA contains

90 a targeting motif. The one known example of dominant escape derives from the host
91 interleukin-6 (IL-6) transcript [26,27,29].

92 IL-6 expression is required for survival of B cells infected with KSHV, and the virus
93 engages a number of strategies to drive production of this cytokine [30-38]. The IL-6 mRNA
94 is directly refractory to SOX cleavage and thus remains robustly induced during host
95 shutoff due to the presence of a specific ‘SOX resistance element’ (SRE) [26,29]. Even in the
96 absence of infection, reporter mRNAs bearing the IL-6 SRE remain stable in SOX-expressing
97 cells, an observation that has helped delineate features of this novel RNA element required
98 for the protective phenotype [26,27]. The IL-6 SRE was fine mapped to a 200 nt sequence
99 within the 3’ UTR, which was subsequently shown to assemble an ‘escape complex’ of at
100 least 8 cellular RNA binding proteins involved in protection [26,27]. How this complex
101 functions to restrict SOX recognition remains largely unknown, although nucleolin (NCL)
102 plays an essential role. NCL is partially relocalized from the nucleolus to the cytoplasm
103 during lytic KSHV infection, where it binds the SRE using its RNA recognition motif and
104 engages in protein-protein interactions related to escape with its carboxyl-terminal RGG
105 domain [27].

106 The IL-6 SRE is the first described ribonuclease escape element and much remains to
107 be learned about its function, as well as whether other related elements exist that protect
108 their associated mRNA. Here, we reveal that the IL-6 SRE is broadly protective against a
109 diverse group of viral endonucleases, suggesting an underlying commonality in the
110 mechanism by which these host shutoff factors recognize their mRNA targets. It is not
111 indiscriminately protective, however, as host quality control endonucleases are not
112 blocked by the IL-6 SRE. We then identify a second, novel SRE within the GADD45B mRNA,

113 which displays some physical and functional similarities to the IL-6 SRE. Collectively, these
114 findings suggest that a diversity of nuclease escape elements exist, and that their
115 characterization may lead to new insights into the control of mRNA fate in both infected
116 and uninfected cells.

117

118

119 **RESULTS**

120 **The IL-6 derived resistance element broadly protects against cleavage by viral but** 121 **not cellular endonucleases**

122 The 3' UTR of IL-6 contains a transferrable 200 nt SRE that protects its associated mRNA
123 from SOX-induced degradation [26,27]. The SRE also protects mRNA from cleavage by the
124 unrelated vhs endonuclease encoded by herpes simplex virus type 1 (HSV-1), hinting that
125 this RNA element may restrict endonuclease targeting in a broader capacity [27]. To test
126 this hypothesis, we assessed whether the presence of the SRE impacted the ability of a
127 panel of homologous and heterologous mRNA-specific viral endonucleases to degrade a
128 target mRNA. In addition to HSV-1 vhs, these included homologs of KSHV SOX from the
129 related gammaherpesviruses Epstein-Barr virus (EBV; BGLF5) and murine
130 gammaherpesvirus 68 (MHV68; muSOX), as well as the heterologous host shutoff
131 endonuclease from influenza A virus (IAV; PA-X) [3,17,39]. As anticipated, the control GFP
132 mRNA was readily degraded in 293T cells co-transfected with plasmids expressing each of
133 the viral endonucleases as measured by RT-qPCR (**Fig. 1A**). However, addition of the IL-6
134 derived SRE to the 3' UTR of GFP (GFP-IL-6-SRE) prevented each of the viral endonucleases
135 from degrading this mRNA (**Fig. 1B**). Fusion of a size matched segment of the IL-6 3' UTR
136 lacking the SRE to GFP (GFP-IL-6 Δ SRE) reinstated cleavage of the GFP reporter by the viral
137 endonucleases (**Fig. 1B**). These data confirm that the protection conferred by the SRE is
138 not specific to SOX-induced cleavage, but functions more broadly to restrict mRNA cleavage
139 by a diverse set of mammalian virus host shutoff endonucleases.

140 Cleavage sites for IAV PA-X have yet to be determined, but the other endonucleases
141 do not appear to target mRNA in the same location or using the same sequence features,

142 including the SOX homologs [1,9,21,40,41]. Thus, the IL-6 derived SRE is unlikely to
143 function through steric occlusion of a common cleavage site. We instead considered the
144 possibility that the SRE functions like an RNA 'zip code', directing its associated transcript
145 to a location in the cell inaccessible to endonucleases. To test this hypothesis, we used RNA
146 fluorescence *in situ* hybridization (FISH) to monitor how the presence of the IL-6 SRE
147 impacted the localization of its associated mRNA. Six phage MS2-derived stem-loops were
148 introduced upstream of the SRE or Δ SRE segment of the IL-6 3' UTR in the pcDNA3
149 luciferase reporter, enabling visualization of the RNA in transfected 293T cells using a Cy3-
150 labeled RNA probe directed against the MS2 sequences [42]. There was no distinguishable
151 difference in the localization of the SRE and Δ SRE containing mRNAs, both of which were
152 present relatively diffusely throughout the cell (**Fig. 1C**). The FISH signal was specific to
153 transfected cells, as we observed no fluorescence in neighboring untransfected cells nor
154 autofluorescence from transfected cells lacking the Cy3 probes (**Fig. 1C**). Although these
155 data do not exclude the possibility that the SRE-containing transcript became sequestered
156 into micro-aggregates or other structures not visible at this level of resolution, they do not
157 support relocalization as the driver of escape from viral endonuclease cleavage.

158
159 We next considered whether the inability to cleave an IL-6 SRE-containing
160 transcript was specific to viral endonucleases or similarly extended to host endonucleases.
161 Although basal cellular mRNA decay is carried out by exonucleases, host quality control
162 pathways involve endonucleases to promote rapid clearance of aberrant mRNA [43-45].
163 We applied two strategies to monitor the activity of the SRE against host endonucleases.
164 The first was to use a nonsense mediated decay (NMD) target containing a premature

165 termination codon (PTC) 100 amino acids into the body of an RFP reporter mRNA (dsRed2-
166 PTC) [10]. The NMD pathway detects PTCs during translation and directs cleavage of the
167 mRNA by the Smg6 endonuclease [46]. Depletion of Smg6 from 293T cells using siRNAs
168 restored dsRed2-PTC mRNA levels to those of the control dsRed2 transcript, confirming
169 that this was an NMD substrate degraded by Smg6 (**Fig. 2A-B**). We then fused the IL-6
170 derived SRE to the 3' UTR of dsRed2-PTC (dsRed2-PTC-SRE) or, as a control, the size
171 matched region from the IL-6 3' UTR lacking the SRE (dsRed2-PTC- Δ SRE) and measured
172 the levels of each mRNA by RT-qPCR in 293T cells (**Fig. 2C**). In contrast to the viral
173 endonucleases, the SRE did not impair Smg6-mediated cleavage of its target mRNA, as all
174 three PTC-containing transcripts were similarly degraded (**Fig. 2A & 2C**).

175 The second strategy to monitor host endonuclease activity was to express the nsp1
176 protein from SARS coronavirus. Nsp1 is not itself a nuclease, but it binds the 40S ribosome
177 and causes it to stall on the mRNA, thus activating cleavage of the mRNA by an as yet
178 unknown cellular endonuclease via a mechanism reminiscent of no-go decay [47,48].
179 Although the endonuclease involved in this pathway has not been established, it is known
180 not to be Smg6 and thus this enabled evaluation of a distinct host endonuclease [48]. Nsp1
181 was co-transfected with the GFP-SRE or GFP- Δ SRE reporter into 293T cells, and depletion
182 of the GFP transcript was measured by RT-qPCR. Similar to the NMD substrate, the SRE did
183 not prevent degradation of the GFP mRNA in nsp1-expressing cells (**Fig. 2D**). Collectively,
184 these results suggest that the IL-6 derived SRE confers broad protection against viral but
185 not cellular endonucleases. Given that the host endonucleases require ongoing translation
186 for target recognition, these data also confirm that the SRE does not pull its associated
187 mRNA out of the translation pool.

188

189 **GADD45B mRNA is also resistant to SOX-induced degradation.**

190 To determine whether this property of broad inhibition of viral endonucleases was
191 restricted to the IL-6 SRE, we sought to identify other SRE-bearing transcript(s). Based on
192 our previous finding that the IL-6 SRE required binding by a complex of cellular proteins
193 including NCL, we mined a published RNAseq dataset for transcripts that were not
194 depleted in SOX expressing 293T cells and were known to be bound by NCL [22,49-51]. A
195 transcript that fit these criteria was growth arrest and DNA damage-inducible 45 beta
196 (GADD45B). Notably, the GADD45B mRNA was also previously shown to escape
197 degradation in HSV-1 vhs-expressing cells, further suggesting it might contain an SRE [52-
198 54]. We first examined whether the GADD45B mRNA was resistant to host shutoff upon
199 lytic reactivation of a KSHV-positive B cell line (TREX-BCBL1) and a renal carcinoma cell
200 line stably expressing the KSHV BAC16 (iSLK.219). Both TREX-BCBL1 and iSLK.219 cells
201 harbor a doxycycline (dox)-inducible version of the major viral lytic transactivator RTA
202 that promotes entry into the lytic cycle upon dox treatment [55,56]. Unlike the GAPDH
203 mRNA, which is degraded by SOX upon lytic reactivation, the GADD45B mRNA levels
204 remained unchanged both in reactivated TREX-BCBL1 and iSLK.219 cells as measured by
205 RT-qPCR (**Fig. 3A & 3B**). We also confirmed that, unlike the GAPDH mRNA, the endogenous
206 GADD45B mRNA was not depleted upon transfection of KSHV SOX or HSV-1 vhs into 293T
207 cells (**Fig. 3C**).

208 Recently, we showed that KSHV SOX cleaves its targets at a specific but degenerate
209 RNA motif [21]. Thus, the failure of SOX (or perhaps vhs) to degrade the GADD45B mRNA
210 could either be due to the absence of such a targeting motif (e.g. passive escape), or to the

211 presence of a specific protective element like the IL-6 SRE (e.g. dominant escape). To
212 distinguish these possibilities, we constructed chimeras between GFP, which has a well-
213 characterized SOX cleavage element, and the GADD45B 5' UTR, 3' UTR, or coding region
214 (CDS) (**Fig. 3D**). Co-transfection of the GFP-fused GADD45 3' UTR construct with SOX into
215 293T cells did not lead to degradation of this mRNA, whereas the GFP-GADD45 5' UTR or
216 CDS fusions were readily degraded in SOX-expressing cells (**Fig. 3E**). Thus, similar to the
217 IL-6 3' UTR, the GADD45B 3' UTR contains a protective sequence that prevents SOX
218 cleavage of an established target mRNA.

219
220 **Hairpin structures within the GADD45B and IL-6 SREs are important for conferring**
221 **resistance to SOX cleavage**

222 To refine which GADD45B sequence encompassed the SRE, we initially looked for
223 similarities between the GADD45B 3' UTR and the IL-6 SRE using Clustal W alignment.
224 While there were no stretches of significant sequence identity between the two RNAs, the
225 last ~200nt of the GADD45B 3'UTR had the highest similarity (~46%) to the IL-6 SRE (**Fig.**
226 **S1**). We therefore fused this putative SRE segment of the GADD45B 3' UTR to GFP
227 (GADD45B-SRE), and found that it was sufficient to confer nearly the same level of
228 protection from SOX as the full GADD45B 3' UTR in transfected 293T cells (**Fig. 4A**). Thus,
229 similar to IL-6, the GADD45B 3' UTR contains a ~200 nt SRE (henceforth termed G-SRE).

230 We next sought to determine whether these two SREs could adopt a common
231 secondary structure. RNAfold-based predictions showed that the 3'-most segment of both
232 SREs form a long stem-loop protruding structure with at least one bulge near the middle of
233 the stem, whereas the other regions of the SREs did not fold into any similar high-

234 confidence structures (**Fig. 4B**). To validate this predicted SRE stem loop structure
235 experimentally, we applied in-line probing, an RNA cleavage assay in which base-paired or
236 structurally constrained nucleotides are protected from spontaneous phosphodiester bond
237 hydrolysis [57]. Results from the cleavage reaction (**Fig. S2**) largely confirmed the RNAfold
238 predictions, apart from a small variation in the IL-6 hairpin. We then tested whether this
239 structure is required for either IL-6 SRE or G-SRE function by changing two conserved TT
240 nucleotides located directly adjacent to the bulge in each hairpin structure to GG (SRE_GG;
241 mutated residues marked with asterisks Fig. 4B). We also separately mutated the AA
242 residues predicted to base pair with these nucleotides on the other side of the loop to CC
243 (SRE_CC). Both the SRE_GG and the SRE_CC mutations in the IL-6 or GADD45B GFP fusions
244 resulted in partial degradation of these mRNAs upon SOX expression in 293T cells,
245 suggesting that disruption of that portion of the SRE hairpin impaired the protective
246 capacity of each SRE (**Fig. 4C & 4D**). Notably, combining these mutations together
247 (SRE_GG+CC), which should restore the secondary structure of the stem-loop, rescued the
248 fully protective phenotype in SOX expressing cells (**Fig. 4C & 4D**). This suggests that, at
249 least for this region of each SRE, RNA structure rather than the specific sequence is
250 important for protection against SOX cleavage.

251 **The GADD45B and IL-6 SREs assemble a partially overlapping ribonucleoprotein** 252 **complex**

253 We previously determined that the IL-6 SRE assembles a specific ribonucleoprotein
254 (RNP) 'escape' complex that is critical for its ability to mediate protection from cleavage by
255 SOX [26,27]. Given the partial similarities in length, sequence, and structure between the
256 IL-6 SRE and the G-SRE, we hypothesized that they might also assemble a similar set of

257 RNPs to mediate their protective function. Indeed, it had already been established that both
258 transcripts bind NCL [27,49]. We therefore performed Comprehensive Identification of
259 RNA binding Proteins (ChIRP) to evaluate whether the set of proteins required for IL-6 SRE
260 function were similarly bound *in vivo* to the GADD45 3'UTR (**Fig. 5A**). Briefly, ChIRP
261 involves purifying an RNA of interest along with its associated proteins from crosslinked,
262 sonicated cells using specific RNA probe-based capture [58]. Proteins bound to the
263 GADD45 3' UTR in transfected 293T cells were identified by Western blot following ChIRP
264 (**Fig. 5B**). We recovered NCL and HuR (also known as ELAVL1), two proteins that were
265 previously identified as important for IL-6 escape from SOX degradation [26,27]. We also
266 identified hnRNPU, a protein that binds the IL-6 SRE but is not required for escape of the
267 IL-6 SRE from SOX [27]. However, other IL-6 SRE-bound proteins required for its escape
268 function were absent from the GADD45 3' UTR, including IGF2BP1, STAU1, ZC3HAV1,
269 YTHDC2, NPM1, and hnRNPD.

270 To further validate the interactions with NCL, HuR, and hnRNPU, we
271 immunoprecipitated (IP) each endogenous protein from 293T cells and performed RT-qPCR
272 to measure the level of co-precipitating endogenous GADD45 RNA. We observed a >5-fold
273 enrichment of GADD45 mRNA over the mock (IgG) IP for both NCL and HuR, although we
274 were not able to detect an association with hnRNPU in this assay (data not shown) (**Fig.**
275 **4C**). We confirmed that the interaction occurs on the GADD45 3'UTR by performing the IPs
276 from cells transfected with a GFP reporter fused to either the GADD45 5' UTR or 3' UTR
277 (**Fig. 4D**). Collectively, these data suggest that while there is some overlap between the
278 sequence, structure, and RNA binding proteins associated with the GADD45 and IL-6 SREs,

279 these elements likely assemble distinct RNP complexes and thus may function in a related
280 but non-identical manner.

281

282

283 **The GADD45 and IL-6 SREs share a requirement for HuR but differ in the breadth of**
284 **their protective capacity**

285 Depletion of either HuR or NCL impairs the ability of the IL-6 derived SRE to protect
286 its associated mRNA from degradation by SOX [26,27]. Given that both proteins are also
287 bound by the G-SRE, we evaluated whether they were similarly important for G-SRE-
288 mediated escape. We individually depleted each protein from 293T cells using siRNAs
289 targeting HuR or NCL (or control non-targeting siRNAs), then measured the ability of SOX
290 to degrade the GFP-GADD45-3'UTR reporter by RT-qPCR (**Fig. 6A & 6B**). Similar to the IL-6
291 SRE, depletion of HuR eliminated the protective capacity of the G-SRE, leading to
292 degradation of the GFP-GADD45-3'UTR mRNA in SOX-expressing cells (**Fig. 6A**).
293 Surprisingly however, depletion of NCL did not impair the protective effect of the G-SRE in
294 SOX-expressing cells (**Fig. 6B**).

295 Finally, we used the GFP-GADD45-3'UTR reporter to evaluate whether the G-SRE
296 conferred protection from cleavage by the panel of viral endonucleases described in Fig. 1.
297 Using the same experimental set up as was used for the IL-6 derived SRE reporter, we
298 observed that while the GADD45 3' UTR protected against SOX and vhs, it was unable to
299 protect against degradation by muSOX, BGLF5, and PA-X (**Fig. 6C**). Furthermore, it did not
300 protect against cleavage by the nsp1-activated host endonuclease (**Fig. 6C**). Thus, although
301 the IL-6 and GADD45B derived nuclease escape elements exhibit a number of similarities,

302 they are distinct in both their RNP complex requirements and in the breadth of nucleases
303 they restrict.

304

305 **DISCUSSION**

306 Viruses extensively interface with the host gene expression machinery to promote
307 their own RNA and protein synthesis and to control the cellular response to infection. In
308 this regard, they have proven to be invaluable tools to dissect mechanisms of gene
309 regulation. Here, we reveal that a ~200 nt sequence present in the 3' UTR of the cellular IL-
310 6 mRNA functions as a broad-acting, virus-specific endonuclease escape element, and
311 identify a similar element in the GADD45B 3' UTR. Although these two SREs are not
312 identical in their protective capacity, they display some sequence and putative structural
313 similarities and are both functionally dependent on HuR binding. We hypothesize that
314 these may therefore be representative members of a new type of RNA regulatory element
315 engaged during viral endonuclease-triggered mRNA decay. Determining whether other
316 such elements exist in mammalian or viral mRNAs is an important future goal, as is
317 deciphering conditions under which such elements impact RNA fate in uninfected cells.

318 The IL-6 and GADD45B SREs display relatively limited sequence similarity but have
319 at least one structurally important stem-loop in common. Thus, RNA structure appears to
320 be a central component of an SRE and is likely to influence recruitment or arrangement of
321 proteins involved in escape. This is in line with the fact that RNP assembly can be more
322 heavily impacted by structural fidelity than primary sequence recognition [59]. We
323 hypothesize that there is a core set of proteins required for SRE function, such as HuR, but
324 that individual SREs recruit distinct accessory factors that dictate the conditions or

325 mechanism by which that SRE protects against nuclease targeting. This is in agreement
326 with the fact that many of the SRE bound proteins have a breadth of roles in controlling
327 RNA fate beyond conferring nuclease escape [60-64]. SRE activity may be further impacted
328 by the cellular context and neighboring regulatory features, particularly in the case of
329 tightly controlled transcripts. The 3' UTR of IL-6, for example, is targeted by several cellular
330 endonucleases including MCP1P1 [65-67], which has recently been reported to be inhibited
331 during de novo KSHV infection [68]. The above features underscore the importance of
332 characterizing multiple SREs to parse out specific protein requirements, but also present
333 challenges for the identification of SREs, as they cannot be easily predicted. Indeed, it has
334 taken more than a decade from the first report of IL-6 escaping SOX-induced host shutoff to
335 identify a second SRE-containing mRNA [29].

336 The observation that the IL-6 SRE in particular acts against diverse viral
337 endonucleases but does not impact host endonucleases has important implications for
338 understanding target recognition by these host shutoff factors. First, it suggests that there
339 are key commonalities to how the viral endonucleases are recruited to mRNAs, and that
340 these features are distinct from those involved in cellular endonuclease recruitment. The
341 viral endonucleases recognize translation competent mRNAs, but do not require ongoing
342 translation for cleavage [10]. While vhs is recruited to a 5' cap proximal location due to its
343 interaction with a eIF4H, the SOX homologs do not respond to particular location cues on
344 their target mRNA, and instead recognize a degenerate target motif that can be positioned
345 anywhere [10,21,69-71]. PA-X has been suggested to bind RNA processing factors in the
346 nucleus, but how it recognizes cytoplasmic mRNA targets remains unknown [72]. By
347 contrast, the cellular NMD and no-go decay quality control pathways show a clear

348 dependence on translation for target recognition, and mRNA cleavage occurs at the site of
349 the error or translation stall [13]. The observation that neither the IL-6 nor GADD45B SREs
350 impede these cellular endonucleases indicates that SREs are not inhibitory to translation.
351 Furthermore, our FISH data do not support mRNA relocalization or sequestration as a
352 driving feature of SRE-mediated escape. We instead hypothesize that the SRE somehow
353 occludes one or more factors required for recruitment of the viral endonucleases. This
354 could occur via long-range interactions with mRNA cap-associated proteins, which we
355 previously showed can take place for the IL-6 SRE [27]. The fact that the GADD45B SRE
356 restricts against a more limited set of host shutoff factors argues against a single factor
357 requirement. However, it is possible that there are multiple binding sites on one factor that
358 are more comprehensively blocked by the IL-6 SRE. Independent of the mechanisms
359 involved, nuclease escape elements could be developed as tools to broadly inhibit viral
360 endonucleases without disrupting normal RNA decay pathways.

361 How might viruses benefit from maintaining the expression of IL-6 and GADD45
362 during infection? The requirement for IL-6 during KSHV infection is well documented [30-
363 38], but the role of GADD45B may be more nuanced. While we demonstrated that it
364 escapes host shutoff during lytic KSHV infection, GADD45B expression is repressed by viral
365 miRNAs during latency to avoid its cell cycle arrest and pro-apoptotic functions [73].
366 However, GADD45B has a number of additional activities that could be necessary for the
367 viral lytic cycle. These include promoting DNA demethylation and Retinoblastoma (Rb)
368 inactivation, processes that are important for a number of DNA viruses, including KSHV
369 [74-79]. If our hypothesis is correct that there are numerous SREs throughout the
370 transcriptome, it is likely that individual viruses require only a subset of these host genes

371 for replication. Other mRNAs may collaterally escape simply because they contain SREs
372 that functionally mimic those present in the 'required' mRNAs. In this regard, the fact that
373 a given mRNA escapes degradation by multiple viral endonucleases does not necessarily
374 indicate that expression of that gene is broadly required for infection. Finally, it is
375 important to bear in mind that the SREs discovered thus far are cellular elements that
376 assemble cellular proteins—and thus presumably play host-directed roles in the regulation
377 of their associated transcripts. It may therefore be the case that some SRE-bearing mRNAs
378 function in an antiviral capacity. Exploring possible virus-host evolutionary interplay for
379 SREs remains an exciting prospect for future studies.

380

381

382 **MATERIALS AND METHODS**

383 **Cells and transfections.** The KSHV-positive B cell line bearing a doxycycline-inducible
384 version of the major lytic transactivator RTA (TREX-BCBL-1) [55] was maintained in RPMI
385 medium (Invitrogen) supplemented with 10% fetal bovine serum (FBS; Invitrogen), 200
386 μ M L-glutamine (Invitrogen), 100 U/ml penicillin/streptomycin (Invitrogen), and 50 μ g/ml
387 hygromycin B (Omega Scientific). Lytic reactivation was induced by treatment with 20
388 ng/ml 2-O-tetradecanoylphorbol-13-acetate (TPA; Sigma), 1 μ g/ml doxycycline (BD
389 Biosciences), and 500 ng/ml ionomycin (Fisher Scientific) for 48h. 293T cells (ATCC) were
390 grown in DMEM (Invitrogen) supplemented with 10% FBS. The KHSV-infected renal
391 carcinoma cell line iSLK.219 bearing doxycycline-inducible RTA was grown in DMEM
392 supplemented with 10% FBS [56]. KSHV lytic reactivation of the iSLK.219 cells was

393 induced by the addition of 0.2 µg/ml doxycycline (BD Biosciences) and 110 µg/ml sodium
394 butyrate for 48 h.

395 For DNA transfections, cells were plated and transfected after 24h when 70%
396 confluent using linear PEI (polyethylenimine). For small interfering RNA (siRNA)
397 transfections, 293T cells were reverse transfected in 12-well plates by INTERFERin
398 (Polyplus-Transfection) with 10 µM of siRNAs. siRNAs were obtained from IDT as DsiRNA
399 (siRNA SMG6: hs.Ri.SMG6.13.1; siRNA NCL: hs.Ri.NCL.13.1; siRNA HuR ELAVL1#1:
400 hs.Ri.ELAVL1.13.2; siRNA ELAVL1#2: hs.Ri.ELAVL1.13.3). 48h following siRNA
401 transfection, the cells subjected to DNA transfection as indicated.

402

403 **Plasmids.** The GADD45B 5'UTR and CDS were obtained as G-blocks from IDT and cloned
404 into a pcDNA3.1 plasmid downstream of the GFP coding sequence. GADD45B 3'UTR was
405 cloned from a pDest-765 plasmid (kindly provided by J. Ziegelbauer) into a pcDNA3.1
406 plasmid downstream of the GFP coding sequence. The GFP-IL-6 3'UTR, SRE and ΔSRE
407 fusion constructs were described previously [27]. The dsRed2 and dsRed2-PTC reporters
408 were described elsewhere [10]. The SRE and ΔSRE were PCR amplified from the GFP
409 reporters and cloned downstream of the dsRed2 ORF.

410 Point mutations were introduced with the Quickchange site directed mutagenesis
411 protocol (Agilent) using the primers described in **table S1**.

412

413 **FiSH.** Stellaris FiSH probes recognizing MS2 and GAPDH labeled with Quasar 570 Dye
414 (MS2: SMF-1063-5; GAPDH: SMF-2026-1) were hybridized in 293T cells following
415 manufacturer's instructions available online at www.biosearchtech.com/stellarisprotocols.

416 Briefly, 293T cells were grown on coverslips and transfected with either an empty vector
417 control or the MS2-SRE or MS2 Δ SRE constructs. 24h later, cells were washed, fixed in 4%
418 formaldehyde and permeabilized in 70% ethanol. Probes (12.5 μ M) were then hybridized
419 for >5h at 37°C in Vanadyl ribonucleoside (10 μ M), formamide (10%), saline sodium citrate
420 (SSC), dextran (10%) and BSA (0.2%). DAPI was added for the last hour to stain cell nuclei.
421 Coverslips were washed in SSC and mounted in Vectashield mounting medium
422 (VectorLabs) before visualization by confocal microscopy on a Zeiss LSM 710 AxioObserver
423 microscope.

424

425 **Comprehensive Analysis of RNA Binding Proteins (ChIRP).** ChIRP was carried out
426 according to a protocol published previously [58] with minor modifications. Briefly, 293T
427 cells were transfected with the GFP-GADD45 3'UTR plasmid and 24h later cells were
428 crosslinked in 3% formaldehyde for 30 minutes, quenched in 125mM Glycine, washed with
429 PBS and the pellet was flash frozen. Pellets were then lysed in fresh ChIRP Lysis Buffer
430 [Tris pH 7.4 50mM, EDTA 10mM, SDS 1%], sonicated, and cell debris was removed by
431 centrifugation at (14,000rpm for 10 min) Two mL of hybridization buffer was added to
432 each sample along with 100pmol of the indicated probes (see **table S1** for sequences).
433 Hybridization was carried out for 4-12h. After adding streptavidin beads to the samples for
434 1h, samples were washed and reverse crosslinked at 65°C overnight. For western blotting,
435 beads were resuspended in 4X loading buffer, boiled for 30 minutes and resolved by SDS-
436 PAGE.

437

438 **In-line probing.** RNA was synthesized by Dharmacon (SRE-HP #CTM-299208, GADD45-
439 HP- #CTM-299209). Approximately 1ug of RNA was 5' end-labeled and purified on an 8M
440 urea gel. Samples were then ethanol precipitated in presence of glycogen, washed in 70%
441 ethanol and dissolved in 20 μ L of DEPC-treated water. Reactions were carried out with
442 ~1uL of purified RNA (~100,000cpm). In-line probing was performed following a standard
443 procedure [57]. Briefly, in-line probing assays were carried for 40h in 2X in-line buffer
444 [100 mM Tris-HCl, pH 8.3, 40 mM MgCl₂, 200 mM KCl] and quenched by adding the same
445 volume of RNA loading Buffer [95% formamide, 10 mM EDTA and 0.025% xylene cyanol].
446 The no-reaction (NR) treatment, RNase T1 (T1) and partial base hydrolysis (-OH) ladders
447 were prepared as 20 μ L reactions and quenched with 20 μ L RNA loading buffer. Dried gels
448 were exposed on a phosphorimager screen and scanned using a Typhoon laser-scanning
449 system (GE Healthcare).

450

451 **RT-qPCR.** Total RNA was harvested using Trizol following the manufacture's protocol.
452 cDNAs were synthesized from 1 μ g of total RNA using AMV reverse transcriptase
453 (Promega), and used directly for quantitative PCR (qPCR) analysis with the DyNAmo
454 ColorFlash SYBR green qPCR kit (Thermo Scientific). Signals obtained by qPCR were
455 normalized to 18S.

456

457 **RNA Immunoprecipitation.** Cells were crosslinked in 1% formaldehyde for 10 minutes,
458 quenched in 125mM glycine and washed in PBS. Cells were then lysed in low-salt lysis
459 buffer [NaCl 150mM, NP-40 0.5%, Tris pH8 50mM, DTT 1mM, MgCl₂ 3mM containing
460 protease inhibitor cocktail and RNase inhibitor] and sonicated. After removal of cell debris,

461 specific antibodies were added as indicated overnight at 4°C. Magnetic G-coupled beads
462 were added for 1h, washed three times with lysis buffer and twice with high-salt lysis
463 buffer (low-salt lysis buffer except containing 400mM NaCl). Samples were separated into
464 two fractions. Beads containing the fraction used for western blotting were resuspended in
465 30µL lysis buffer. Beads containing the fraction used for RNA extraction were resuspended
466 in Proteinase K buffer (NaCl 100mM, Tris pH 7.4 10mM, EDTA 1mM, SDS 0.5%) containing
467 1µL of PK (Proteinase K). Samples were incubated overnight at 65°C to reverse
468 crosslinking. Samples to be analyzed by western blot were then supplemented with 10µL of
469 4X loading buffer before resolution by SDS-PAGE. RNA samples were resuspend in Trizol
470 and were processed as described above.

471

472 **Western Blotting.** Lysates were resolved by SDS-PAGE and western blotted with the
473 following antibodies at 1:1000 in TBST (Tris-buffered saline, 0.1% Tween 20): rabbit anti-
474 EST1A/SMG6 (Abcam) rabbit anti-NCL (Abcam), rabbit anti-HuR (Millipore), rabbit anti-
475 actin (Abcam), rabbit anti-IGF2BP1 (Abcam), rabbit anti-YTHDC2 (Abcam), rabbit anti-
476 hnRNPU (Abcam), rabbit anti-ZC3HAV1 (Abcam), rabbit anti-hnRNPD (Abcam), rabbit anti-
477 STAU1 (Pierce), or mouse anti-NPM1 (Abcam). Primary antibody incubations were
478 followed by HRP-conjugated goat anti-mouse or goat anti-rabbit secondary antibodies
479 (Southern Biotechnology, 1:5000).

480

481 **Statistical analysis.** All results are expressed as means \pm S.E.M. of experiments
482 independently repeated at least three times. Unpaired Student's t test was used to evaluate

483 the statistical difference between samples. Significance was evaluated with P values as
484 follows: * $p < 0.1$; ** $p < 0.05$; *** $p < 0.01$.

485

486 **ACKNOWLEDGMENTS**

487 We thank members of the Glaunsinger and Coscoy labs for helpful discussions. We also
488 thank Ming Hammond, Debojit Bose and Carolin Vogt for technical advice on in-line
489 probing.

490

491 **FUNDING**

492 This research was supported by NIH grants CA160556 and CA136367
493 (<http://www.nih.gov/>) and a Burroughs Wellcome Investigator in the Pathogenesis of
494 Infectious Diseases Award ([http://www.bwfund.org/grant-programs/infectious-diseases/
495 investigators-in-pathogenesis-of-infectious-disease](http://www.bwfund.org/grant-programs/infectious-diseases/investigators-in-pathogenesis-of-infectious-disease)) to BAG. B.A.G. is an investigator of the
496 Howard Hughes Medical Institute. Funding for open access charge: Howard Hughes
497 Medical Institute and MM is a HHMI Fellow of the Damon Runyon Cancer Research
498 Foundation (DRG- 2207-14) (<http://www.damonrunyon.org/>).

499

500

501

502 **REFERENCES**

503

504

- 505 1. Gaglia MM, Covarrubias S, Wong W, Glaunsinger BA. A common strategy for host RNA
506 degradation by divergent viruses. *J Virol.* 2012;86: 9527–9530.
- 507 2. Rivas HG, Schmaling SK, Gaglia MM. Shutoff of Host Gene Expression in Influenza A
508 Virus and Herpesviruses: Similar Mechanisms and Common Themes. *Viruses.*
509 2016;8: 102.
- 510 3. Jagger BW, Wise HM, Kash JC, Walters K-A, Wills NM, Xiao Y-L, et al. An overlapping
511 protein-coding region in influenza A virus segment 3 modulates the host response.
512 *Science.* 2012;337: 199–204.
- 513 4. Kwong AD, Frenkel N. Herpes simplex virus-infected cells contain a function(s) that
514 destabilizes both host and viral mRNAs. *Proc Natl Acad Sci USA.* 1987;84: 1926–
515 1930.
- 516 5. Kamitani W, Huang C, Narayanan K, Lokugamage KG, Makino S. A two-pronged
517 strategy to suppress host protein synthesis by SARS coronavirus Nsp1 protein. *Nat*
518 *Struct Mol Biol.* 2009;16: 1134–1140.
- 519 6. Parrish S, Moss B. Characterization of a vaccinia virus mutant with a deletion of the
520 D10R gene encoding a putative negative regulator of gene expression. *J Virol.*
521 2006;80: 553–561.
- 522 7. Parrish S, Moss B. Characterization of a second vaccinia virus mRNA-decapping
523 enzyme conserved in poxviruses. *J Virol.* 2007;81: 12973–12978.
- 524 8. Parrish S, Resch W, Moss B. Vaccinia virus D10 protein has mRNA decapping activity,
525 providing a mechanism for control of host and viral gene expression. *Proc Natl Acad*
526 *Sci USA.* 2007;104: 2139–2144.
- 527 9. Elgadi MM, Hayes CE, Smiley JR. The herpes simplex virus vhs protein induces
528 endoribonucleolytic cleavage of target RNAs in cell extracts. *J Virol.* 1999;73: 7153–
529 7164.
- 530 10. Covarrubias S, Gaglia MM, Kumar GR, Wong W, Jackson AO, Glaunsinger BA.
531 Coordinated destruction of cellular messages in translation complexes by the
532 gammaherpesvirus host shutoff factor and the mammalian exonuclease Xrn1. *PLoS*
533 *Pathog.* 2011 7(10): e1002339
- 534 11. Burgess HM, Mohr I. Cellular 5′-3′ mRNA exonuclease Xrn1 controls double-
535 stranded RNA accumulation and anti-viral responses. *Cell Host Microbe.* 2015;17:

- 536 332–344.
- 537 12. Schoenberg DR, Maquat LE. Regulation of cytoplasmic mRNA decay. *Nat Rev Genet.*
538 2012;13: 246–259.
- 539 13. Mühlemann O, Lykke-Andersen J. How and where are nonsense mRNAs degraded in
540 mammalian cells? *RNA Biol.* 2010;7: 28–32.
- 541 14. Doma MK, Parker R. Endonucleolytic cleavage of eukaryotic mRNAs with stalls in
542 translation elongation. *Nature.* 2006;440: 561–564.
- 543 15. Harigaya Y, Parker R. No-go decay: a quality control mechanism for RNA in
544 translation. *Wiley Interdiscip Rev RNA.* 2010;1: 132–141.
- 545 16. Covarrubias S, Richner JM, Clyde K, Lee YJ, Glaunsinger BA. Host shutoff is a
546 conserved phenotype of gammaherpesvirus infection and is orchestrated exclusively
547 from the cytoplasm. *J Virol.* 2009;83: 9554–9566.
- 548 17. Rowe M, Glaunsinger B, van Leeuwen D, Zuo J, Sweetman D, Ganem D, et al. Host
549 shutoff during productive Epstein-Barr virus infection is mediated by BGLF5 and
550 may contribute to immune evasion. *Proc Natl Acad Sci USA.* 2007;104: 3366–3371.
- 551 18. Glaunsinger B, Ganem D. Lytic KSHV infection inhibits host gene expression by
552 accelerating global mRNA turnover. *Mol Cell.* 2004;13: 713–723.
- 553 19. Abernathy E, Clyde K, Yeasmin R, Krug LT, Burlingame A, Coscoy L, et al.
554 Gammaherpesviral gene expression and virion composition are broadly controlled
555 by accelerated mRNA degradation. *PLoS Pathog.* 2014;10: e1003882.
- 556 20. Richner JM, Clyde K, Pezda AC, Cheng BYH, Wang T, Kumar GR, et al. Global mRNA
557 degradation during lytic gammaherpesvirus infection contributes to establishment of
558 viral latency. *PLoS Pathog.* 2011;7: e1002150.
- 559 21. Gaglia MM, Rycroft CH, Glaunsinger BA. Transcriptome-Wide Cleavage Site Mapping
560 on Cellular mRNAs Reveals Features Underlying Sequence-Specific Cleavage by the
561 Viral Ribonuclease SOX. *PLoS Pathog.* 2015;11: e1005305.
- 562 22. Clyde K, Glaunsinger BA. Deep sequencing reveals direct targets of
563 gammaherpesvirus-induced mRNA decay and suggests that multiple mechanisms
564 govern cellular transcript escape. *PLoS ONE.* 2011;6: e19655.
- 565 23. Chandriani S, Ganem D. Host transcript accumulation during lytic KSHV infection
566 reveals several classes of host responses. *PLoS ONE.* 2007;2: e811.
- 567 24. Clyde K, Glaunsinger BA. Getting the message direct manipulation of host mRNA
568 accumulation during gammaherpesvirus lytic infection. *Adv Virus Res.* 2010;78: 1–
569 42.

- 570 25. Lee YJ, Glaunsinger BA. Aberrant herpesvirus-induced polyadenylation correlates
571 with cellular messenger RNA destruction. *PLoS Biol.* 2009;7: e1000107.
- 572 26. Hutin S, Lee Y, Glaunsinger BA. An RNA element in human interleukin 6 confers
573 escape from degradation by the gammaherpesvirus SOX protein. *J Virol.* 2013;87:
574 4672–4682.
- 575 27. Muller M, Hutin S, Marigold O, Li KH, Burlingame A, Glaunsinger BA. A
576 ribonucleoprotein complex protects the interleukin-6 mRNA from degradation by
577 distinct herpesviral endonucleases. *PLoS Pathog.* 2015;11: e1004899.
- 578 28. Abernathy E, Gilbertson S, Alla R, Glaunsinger B. Viral Nucleases Induce an mRNA
579 Degradation-Transcription Feedback Loop in Mammalian Cells. *Cell Host Microbe.*
580 2015;18: 243–253.
- 581 29. Glaunsinger B, Ganem D. Highly selective escape from KSHV-mediated host mRNA
582 shutoff and its implications for viral pathogenesis. *J Exp Med.* 2004;200: 391–398.
- 583 30. Sin S-H, Roy D, Wang L, Staudt MR, Fakhari FD, Patel DD, et al. Rapamycin is
584 efficacious against primary effusion lymphoma (PEL) cell lines in vivo by inhibiting
585 autocrine signaling. *Blood.* 2007;109: 2165–2173.
- 586 31. Miles SA, Rezai AR, Salazar-González JF, Vander Meyden M, Stevens RH, Logan DM, et
587 al. AIDS Kaposi sarcoma-derived cells produce and respond to interleukin 6. *Proc*
588 *Natl Acad Sci USA.* 1990;87: 4068–4072.
- 589 32. Screpanti I, Musiani P, Bellavia D, Cappelletti M, Aiello FB, Maroder M, et al.
590 Inactivation of the IL-6 gene prevents development of multicentric Castleman's
591 disease in C/EBP beta-deficient mice. *J Exp Med.* 1996;184: 1561–1566.
- 592 33. Leger-Ravet MB, Peuchmaur M, Devergne O, Audouin J, Raphael M, Van Damme J, et
593 al. Interleukin-6 gene expression in Castleman's disease. *Blood.* 1991;78: 2923–2930.
- 594 34. Xie J, Pan H, Yoo S, Gao S-J. Kaposi's sarcoma-associated herpesvirus induction of AP-
595 1 and interleukin 6 during primary infection mediated by multiple mitogen-activated
596 protein kinase pathways. *J Virol.* 2005;79: 15027–15037.
- 597 35. An J, Sun Y, Sun R, Rettig MB. Kaposi's sarcoma-associated herpesvirus encoded
598 vFLIP induces cellular IL-6 expression: the role of the NF-kappaB and JNK/AP1
599 pathways. *Oncogene.* 2003;22: 3371–3385.
- 600 36. Santarelli R, Gonnella R, Di Giovenale G, Cuomo L, Capobianchi A, Granato M, et al.
601 STAT3 activation by KSHV correlates with IL-10, IL-6 and IL-23 release and an
602 autophagic block in dendritic cells. *Sci Rep.* 2014;4: 4241.
- 603 37. Deng H, Chu JT, Rettig MB, Martinez-Maza O, Sun R. Rta of the human herpesvirus
604 8/Kaposi sarcoma-associated herpesvirus up-regulates human interleukin-6 gene

- 605 expression. *Blood*. 2002;100: 1919–1921.
- 606 38. McCormick C, Ganem D. The kaposin B protein of KSHV activates the p38/MK2
607 pathway and stabilizes cytokine mRNAs. *Science*. 2005;307: 739–741.
- 608 39. Oishi K, Yamayoshi S, Kawaoka Y. Mapping of a Region of the PA-X Protein of
609 Influenza A Virus That Is Important for Its Shutoff Activity. *J Virol*. 2015;89: 8661–
610 8665.
- 611 40. Smiley JR, Elgadi MM, Saffran HA. Herpes simplex virus vhs protein. *Meth Enzymol*.
612 2001;342: 440–451.
- 613 41. Everly DN, Feng P, Mian IS, Read GS. mRNA degradation by the virion host shutoff
614 (Vhs) protein of herpes simplex virus: genetic and biochemical evidence that Vhs is a
615 nuclease. *J Virol*. 2002;76: 8560–8571.
- 616 42. Aizer A, Kalo A, Kafri P, Shraga A, Ben-Yishay R, Jacob A, et al. Quantifying mRNA
617 targeting to P-bodies in living human cells reveals their dual role in mRNA decay and
618 storage. *J Cell Sci*. 2014;127: 4443–4456.
- 619 43. Abernathy E, Glaunsinger B. Emerging roles for RNA degradation in viral replication
620 and antiviral defense. *Virology*. 2015;479-480: 600–608.
- 621 44. Isken O, Maquat LE. Quality control of eukaryotic mRNA: safeguarding cells from
622 abnormal mRNA function. *Genes Dev*. 2007;21: 1833–1856.
- 623 45. Schoenberg DR. Mechanisms of endonuclease-mediated mRNA decay. *Wiley*
624 *Interdiscip Rev RNA*. 2011;2: 582–600.
- 625 46. Eberle AB, Lykke-Andersen S, Mühlemann O, Jensen TH. SMG6 promotes
626 endonucleolytic cleavage of nonsense mRNA in human cells. *Nat Struct Mol Biol*.
627 2009;16: 49–55.
- 628 47. Narayanan K, Ramirez SI, Lokugamage KG, Makino S. Coronavirus nonstructural
629 protein 1: Common and distinct functions in the regulation of host and viral gene
630 expression. *Virus Res*. 2015;202: 89–100.
- 631 48. Huang C, Lokugamage KG, Rozovics JM, Narayanan K, Semler BL, Makino S. SARS
632 coronavirus nsp1 protein induces template-dependent endonucleolytic cleavage of
633 mRNAs: viral mRNAs are resistant to nsp1-induced RNA cleavage. *PLoS Pathog*.
634 2011;7: e1002433.
- 635 49. Zhang Y, Bhatia D, Xia H, Castranova V, Shi X, Chen F. Nucleolin links to arsenic-
636 induced stabilization of GADD45alpha mRNA. *Nucleic Acids Res*. 2006;34: 485–495.
- 637 50. Zhang D, Liang Y, Xie Q, Gao G, Wei J, Huang H, et al. A novel post-translational
638 modification of nucleolin, SUMOylation at Lys-294, mediates arsenite-induced cell

- 639 death by regulating gadd45 α mRNA stability. *J Biol Chem.* 2015;290: 4784–4800.
- 640 51. Zheng X, Zhang Y, Chen Y-Q, Castranova V, Shi X, Chen F. Inhibition of NF-kappaB
641 stabilizes gadd45alpha mRNA. *Biochem Biophys Res Commun.* 2005;329: 95–99.
- 642 52. Esclatine A, Taddeo B, Evans L, Roizman B. The herpes simplex virus 1 UL41 gene-
643 dependent destabilization of cellular RNAs is selective and may be sequence-specific.
644 *Proc Natl Acad Sci USA.* 2004;101: 3603–3608.
- 645 53. Barzilai A, Zivony-Elbom I, Sarid R, Noah E, Frenkel N. The herpes simplex virus type
646 1 vhs-UL41 gene secures viral replication by temporarily evading apoptotic cellular
647 response to infection: Vhs-UL41 activity might require interactions with elements of
648 cellular mRNA degradation machinery. *J Virol.* 2006;80: 505–513.
- 649 54. Khodarev NN, Advani SJ, Gupta N, Roizman B, Weichselbaum RR. Accumulation of
650 specific RNAs encoding transcriptional factors and stress response proteins against a
651 background of severe depletion of cellular RNAs in cells infected with herpes simplex
652 virus 1. *Proc Natl Acad Sci USA.* 1999;96: 12062–12067.
- 653 55. Nakamura H, Lu M, Gwack Y, Souvlis J, Zeichner SL, Jung JU. Global changes in
654 Kaposi's sarcoma-associated virus gene expression patterns following expression of
655 a tetracycline-inducible Rta transactivator. *J Virol.* 2003;77: 4205–4220.
- 656 56. Myoung J, Ganem D. Generation of a doxycycline-inducible KSHV producer cell line of
657 endothelial origin: maintenance of tight latency with efficient reactivation upon
658 induction. *J Virol Methods.* 2011;174: 12–21.
- 659 57. Regulski EE, Breaker RR. In-line probing analysis of riboswitches. *Methods Mol Biol.*
660 2008;419: 53–67.
- 661 58. Chu C, Zhang QC, da Rocha ST, Flynn RA, Bharadwaj M, Calabrese JM, et al. Systematic
662 discovery of Xist RNA binding proteins. *Cell.* 2015;161: 404–416.
- 663 59. Bevilacqua PC, Ritchey LE, Su Z, Assmann SM. Genome-Wide Analysis of RNA
664 Secondary Structure. *Annu Rev Genet.* 2016;50: 235–266.
- 665 60. Dean JLE, Sully G, Clark AR, Saklatvala J. The involvement of AU-rich element-binding
666 proteins in p38 mitogen-activated protein kinase pathway-mediated mRNA
667 stabilisation. *Cell Signal.* 2004;16: 1113–1121.
- 668 61. Abdelmohsen K, Gorospe M. RNA-binding protein nucleolin in disease. *RNA Biol.*
669 2012;9: 799–808.
- 670 62. Bell JL, Wächter K, Mühleck B, Pazaitis N, Köhn M, Lederer M, et al. Insulin-like
671 growth factor 2 mRNA-binding proteins (IGF2BPs): post-transcriptional drivers of
672 cancer progression? *Cell Mol Life Sci.* 2013;70: 2657–2675.

- 673 63. White EJF, Brewer G, Wilson GM. Post-transcriptional control of gene expression by
674 AUF1: mechanisms, physiological targets, and regulation. *Biochim Biophys Acta*.
675 2013;1829: 680–688.
- 676 64. Park E, Maquat LE. Staufen-mediated mRNA decay. *Wiley Interdiscip Rev RNA*.
677 2013;4: 423–435.
- 678 65. Matsushita K, Takeuchi O, Standley DM, Kumagai Y, Kawagoe T, Miyake T, et al.
679 Zc3h12a is an RNase essential for controlling immune responses by regulating mRNA
680 decay. *Nature*. 2009;458: 1185–1190.
- 681 66. Paschoud S, Dogar AM, Kuntz C, Grisoni-Neupert B, Richman L, Kühn LC.
682 Destabilization of interleukin-6 mRNA requires a putative RNA stem-loop structure,
683 an AU-rich element, and the RNA-binding protein AUF1. *Mol Cell Biol*. 2006;26:
684 8228–8241.
- 685 67. Mino T, Murakawa Y, Fukao A, Vandenbon A, Wessels H-H, Ori D, et al. Regnase-1 and
686 Roquin Regulate a Common Element in Inflammatory mRNAs by Spatiotemporally
687 Distinct Mechanisms. *Cell*. 2015;161: 1058–1073.
- 688 68. Happel C, Ramalingam D, Ziegelbauer JM. Virus-Mediated Alterations in miRNA
689 Factors and Degradation of Viral miRNAs by MCP1P1. *PLoS Biol*. 2016;14: e2000998.
- 690 69. Feng P, Everly DN, Read GS. mRNA decay during herpes simplex virus (HSV)
691 infections: protein-protein interactions involving the HSV virion host shutoff protein
692 and translation factors eIF4H and eIF4A. *J Virol*. 2005;79: 9651–9664.
- 693 70. Page HG, Read GS. The virion host shutoff endonuclease (UL41) of herpes simplex
694 virus interacts with the cellular cap-binding complex eIF4F. *J Virol*. 2010;84: 6886–
695 6890.
- 696 71. Feng P, Everly DN, Read GS. mRNA decay during herpesvirus infections: interaction
697 between a putative viral nuclease and a cellular translation factor. *J Virol*. 2001;75:
698 10272–10280.
- 699 72. Khaperskyy DA, Schmaling S, Larkins-Ford J, McCormick C, Gaglia MM. Selective
700 Degradation of Host RNA Polymerase II Transcripts by Influenza A Virus PA-X Host
701 Shutoff Protein. *PLoS Pathog*. 2016;12: e1005427.
- 702 73. Liu X, Happel C, Ziegelbauer JM. Kaposi's Sarcoma-Associated Herpesvirus
703 MicroRNAs Target GADD45B To Protect Infected Cells from Cell Cycle Arrest and
704 Apoptosis. *J Virol*. 2017;91: e02045–16.
- 705 74. Cho HJ, Park S-M, Hwang EM, Baek KE, Kim I-K, Nam I-K, et al. Gadd45b mediates
706 Fas-induced apoptosis by enhancing the interaction between p38 and
707 retinoblastoma tumor suppressor. *J Biol Chem*. 2010;285: 25500–25505.

- 708 75. Hume AJ, Kalejta RF. Regulation of the retinoblastoma proteins by the human
709 herpesviruses. *Cell Div.* 2009;4: 1.
- 710 76. Godden-Kent D, Talbot SJ, Boshoff C, Chang Y, Moore P, Weiss RA, et al. The cyclin
711 encoded by Kaposi's sarcoma-associated herpesvirus stimulates cdk6 to
712 phosphorylate the retinoblastoma protein and histone H1. *J Virol.* 1997;71: 4193–
713 4198.
- 714 77. Chang Y, Moore PS, Talbot SJ, Boshoff CH, Zarkowska T, Godden-Kent, et al. Cyclin
715 encoded by KS herpesvirus. *Nature.* 1996;382: 410–410.
- 716 78. Ma DK, Guo JU, Ming G-L, Song H. DNA excision repair proteins and Gadd45 as
717 molecular players for active DNA demethylation. *Cell Cycle.* 2009;8: 1526–1531.
- 718 79. Purushothaman P, Uppal T, Verma SC. Molecular biology of KSHV lytic reactivation.
719 *Viruses.* 2015;7: 116–153.

720

721 **FIGURE LEGENDS**

722 **Figure 1: The IL-6-SRE broadly protects against multiple viral endonucleases. (A)**
723 293T cells were transfected with empty vector (mock) or a plasmid expressing the
724 indicated endonucleases along with a GFP reporter. After 24 h, total RNA was harvested
725 and subjected RT-qPCR to measure GFP mRNA levels. Graphs here and afterwards display
726 individual replicates as dots, together with the mean values (\pm SEM). Statistical significance
727 was determined by the Student t test (* $p < 0.1$; ** $p < 0.05$; *** $p < 0.01$). **(B)** 293T cells were
728 co-transfected with the indicated endonuclease-expressing plasmid expressing together
729 with a GFP-SRE or GFP- Δ SRE reporter. After 24 h, total RNA was harvested and subjected
730 RT-qPCR to measure GFP mRNA levels. **(C)** Top: diagram showing the structure of the
731 reporter mRNA containing MS2 repeats upstream of the SRE or Δ SRE fragment of the IL-6
732 3'UTR. Red lines denote the region detected by the MS2 probe. Bottom: 293T cells were
733 transfected with the indicated MS2 reporters. 24h later, cells were fixed and processed for
734 RNA FISH staining. Signals from the MS2 probes (red) and DAPI stained nuclei (blue) were
735 detected by confocal microscopy.

736
737 **Figure 2: The IL-6-SRE does not protect against cellular endonucleases. (A)** 293T cells
738 were transfected with the indicated dsRed2 reporters. After 24 h, total RNA was harvested
739 and subjected RT-qPCR to measure dsRed mRNA levels. **(B)** 293T cells were treated with
740 siRNAs targeting Smg6 or control non-targeting siRNAs. 48h later, cells were transfected
741 with the indicated dsRed reporters. After 24h, total RNA was harvested and subjected RT-
742 qPCR to measure dsRed mRNA levels (*left*). The efficiency of SMG6 knockdown was
743 measured by western blotting, with actin serving as a loading control (*right*). **(C)** 293T cells
744 were transfected with the indicated dsRed2 reporters. After 24 h, total RNA was harvested
745 and subjected to RT-qPCR to measure dsRed mRNA levels. **(D)** 293T cells were transfected
746 with an empty vector (mock) or a plasmid expressing SCoV nsp1 along with the indicated
747 GFP reporters. After 24 h, total RNA was harvested and subjected RT-qPCR to measure GFP
748 mRNA levels.

749
750 **Figure 3: GADD45B mRNA is protected against SOX degradation. (A, B)** Total RNA was
751 extracted from unreactivated or reactivated KSHV-positive TREG-BCBL-1 (A) cells or
752 iSLK.219 cells (B) and subjected to RT-qPCR to measure endogenous levels of the
753 GADD45B or GAPDH transcript. **(C)** 293T cells were transfected with an empty vector or a
754 plasmid expressing SOX or vhs. After 24 h, total RNA was harvested and subjected to RT-
755 qPCR to measure endogenous levels of GADD45B or GAPDH transcripts. **(D)** Diagram of the
756 reporter constructs where fragments of GADD45B transcript were fused to GFP. **(E)** 293T
757 cells were transfected with the indicated GFP-GADD45B fusion constructs in the presence
758 or absence of a plasmid expressing SOX. After 24 h, total RNA was harvested and subjected
759 to RT-qPCR to measure GFP levels.

760
761 **Figure 4: The SREs contain a long hairpin required for protection against SOX. (A)**
762 293T cells were transfected with the indicated GFP reporter along with a control empty
763 vector (mock) or a plasmid expressing SOX. After 24 h, total RNA was harvested and
764 subjected to RT-qPCR to measure GFP mRNA levels. **(B)** Diagram of the structure
765 prediction obtained with RNAfold for IL-6 and GADD45B SREs. The color scale represents

766 the confidence score of the structure as calculated by RNAfold, with red representing the
767 highest confidence. Asterisks denote the location of mutations that were introduced in the
768 structure for the following assays. The insets are RNAfold predictions of the stem loops of
769 interest in isolation. **(C)** 293T cells were transfected with the indicated GFP reporters
770 containing mutations within IL-6 SRE at the residues marked by a * in (B) along with a
771 control empty vector (mock) or a plasmid expressing SOX. After 24 h, total RNA was
772 harvested and subjected RT-qPCR to measure GFP mRNA levels. **(D)** 293T cells were
773 transfected with the indicated GFP reporters mutated within G- SRE at the residues marked
774 by a * in (B) along with a control empty vector (mock) or a plasmid expressing SOX. After
775 24 h, total RNA was harvested and subjected to RT-qPCR to measure GFP mRNA levels.

776 **Figure 5: The IL-6 and GADD45B SRE bind a partially overlapping set of cellular**
777 **proteins. (A)** Diagram outlining the ChIRP assay. **(B)** 293T were transfected with the GFP-
778 GADD45 3'UTR reporter, then 24h later they were subjected to ChIRP analysis and protein
779 samples were western blotted to assess co-purification of the indicated proteins. **(C)**
780 Crosslinked lysates of 293T cells were subjected to RNA immunoprecipitation (RIP) with
781 control IgG, anti-NCL, or anti-HuR antibodies and the level of co-purifying endogenous
782 GADD45 mRNA was quantified by RT-qPCR. Bars represent the fold enrichment over the
783 mock IP. **(D)** 293T cells were transfected with either the GFP-GADD45 5'UTR or GFP-
784 GADD45 3'UTR reporter for 24 h. Lysates were then subjected to RIP as described in (C).
785 Bars represent the fold enrichment over mock IP.

786
787 **Figure 6: The GADD45 SRE function requires HuR, but is only protective against SOX**
788 **and vhs. (A,B)** 293T cells were treated with siRNAs targeting HuR (A) or NCL (B) or
789 control non targeting siRNAs. 48h later, cells were transfected with the GFP-GADD45-
790 3'UTR reporter along with a control empty vector or a plasmid expressing SOX. After 24 h,
791 total RNA was harvested and subjected to RT-qPCR to measure GFP mRNA levels. Protein
792 levels of HuR and NCL after siRNA-mediated depletion are shown under the bar graphs
793 (~30% and 45% of total protein left respectively) **(C)** 293T cells were transfected with the
794 GFP-GADD45-3'UTR reporter along with a control empty vector or a plasmid expressing
795 the indicated viral endonucleases. After 24 h, total RNA was harvested and subjected to RT-
796 qPCR to measure GFP mRNA levels.

797
798
799

800 SUPPORTING INFORMATION

801

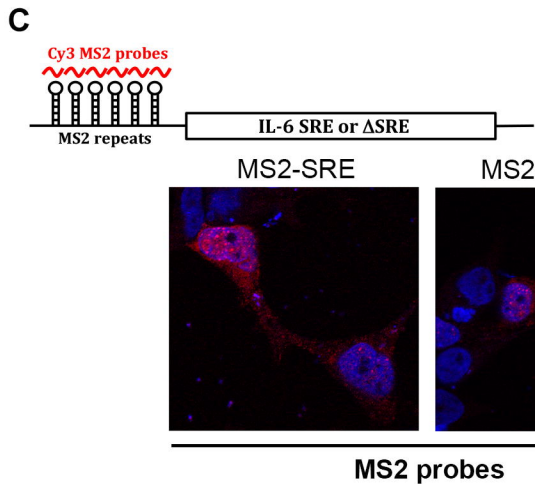
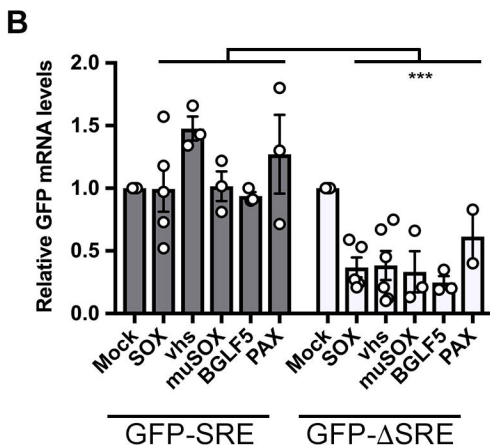
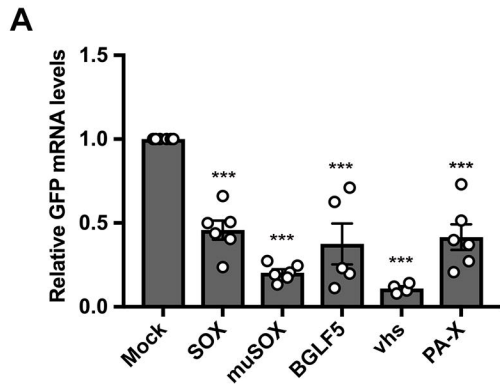
802 **Figure S1:** Clustal W alignment of IL-6 SRE and GADD45B 3'UTR

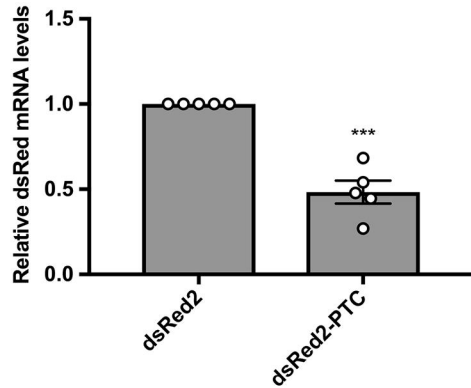
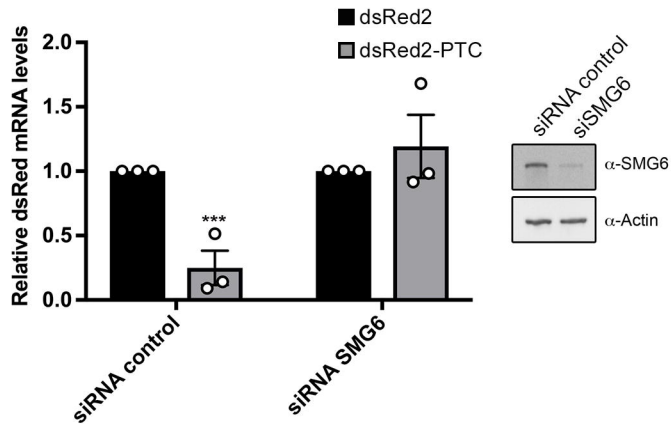
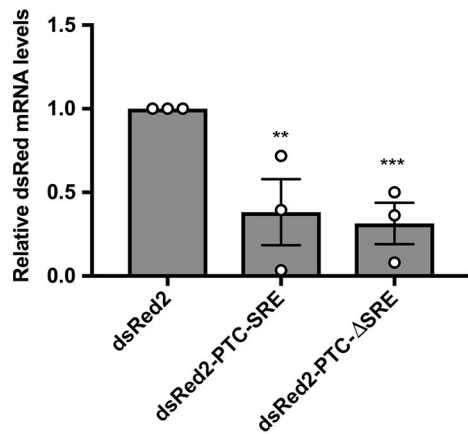
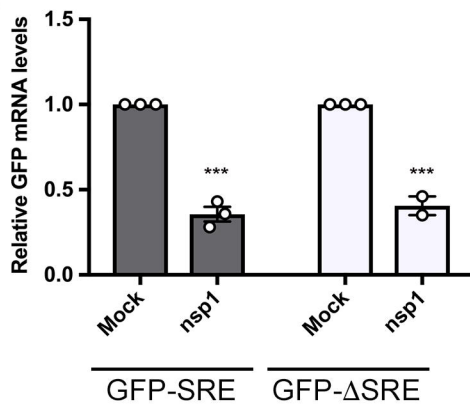
803

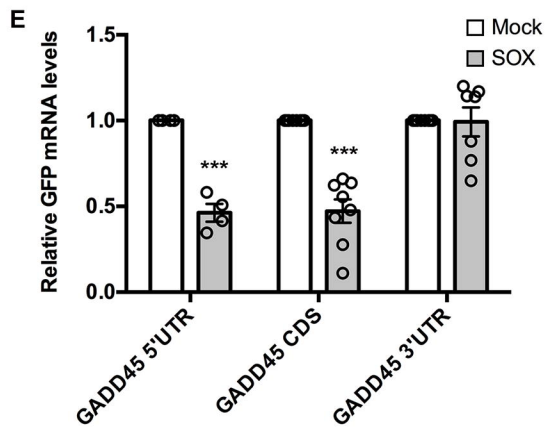
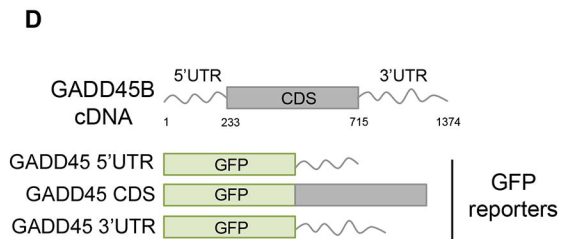
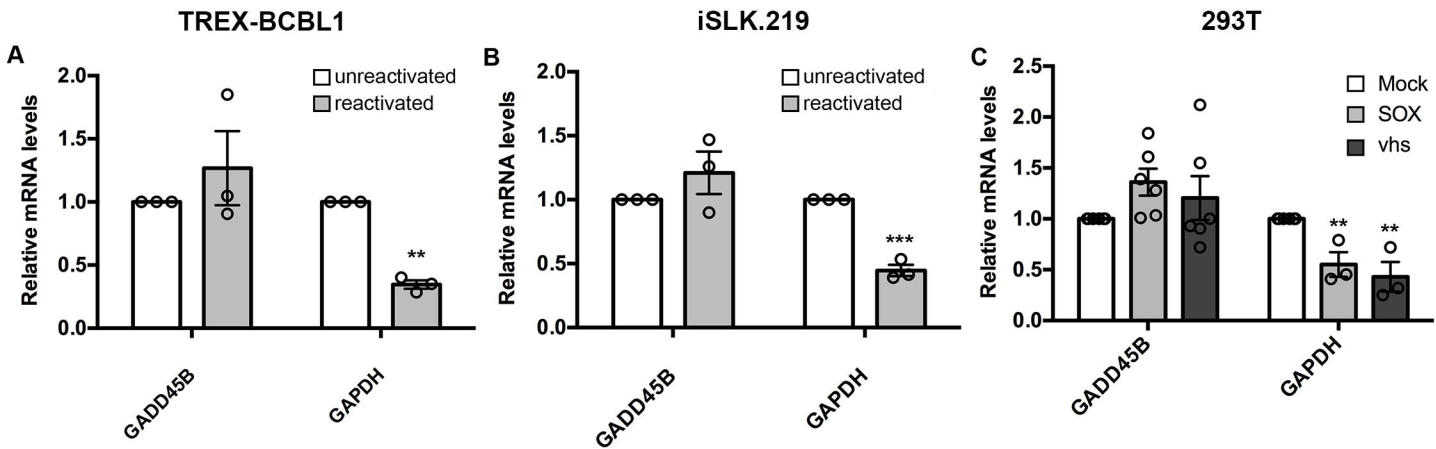
804 **Figure S2:** In-line probing of the IL-6 (left) and GADD45 (right) predicted stem-loop. ³²P-
805 labeled RNA (NR, no reaction) and products resulting from partial digestion with nuclease
806 T1 (T1; cuts after G residues), partial digestion with alkali (-OH), and spontaneous cleavage
807 during a 24h incubation are shown. Product bands corresponding to G residues (generated
808 by T1 digestion) are labeled with black arrows. Predicted paired or unpaired residues are
809 marked on the right of each gel and are shown on the RNA fold diagrams.

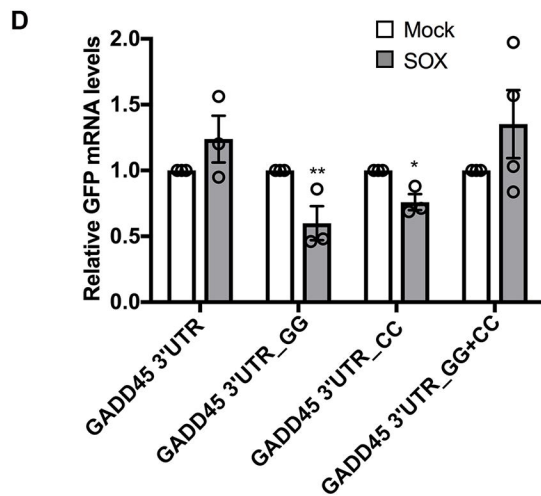
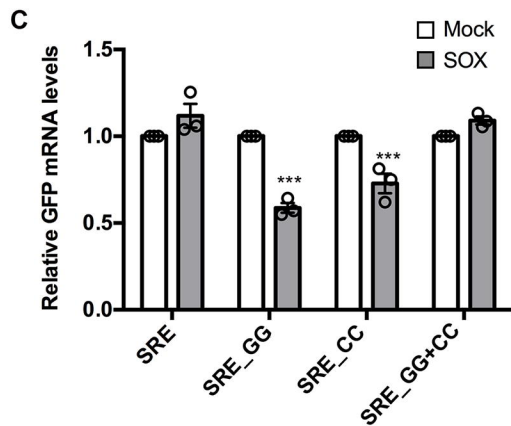
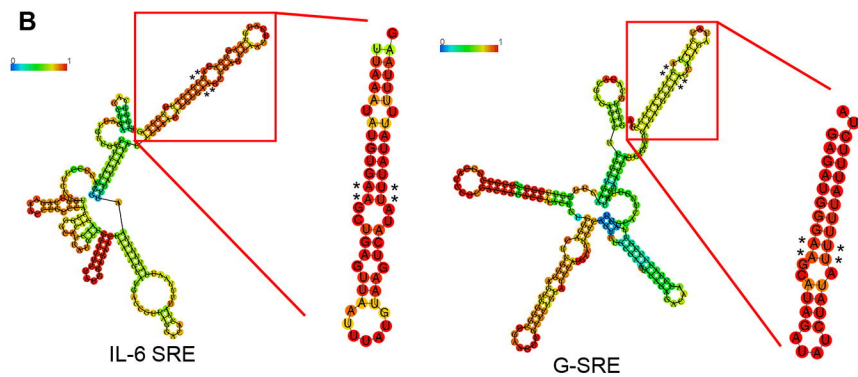
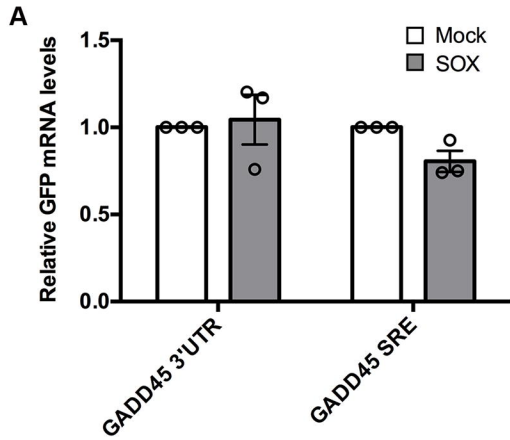
810

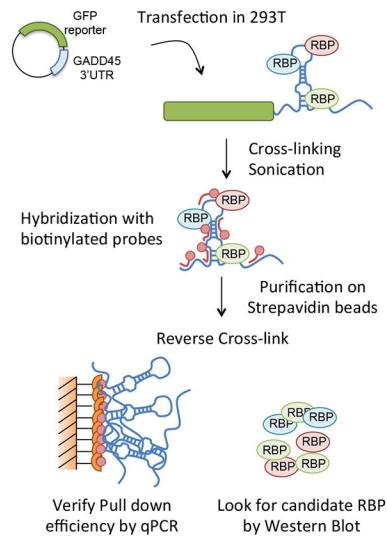
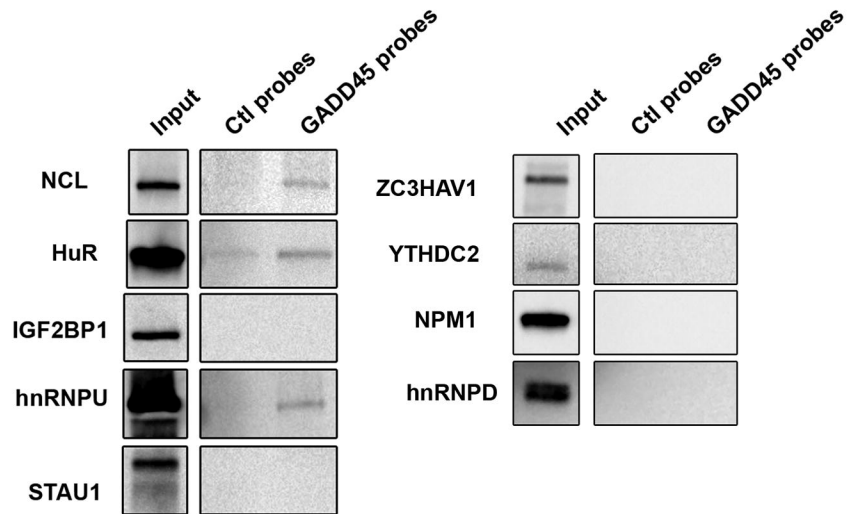
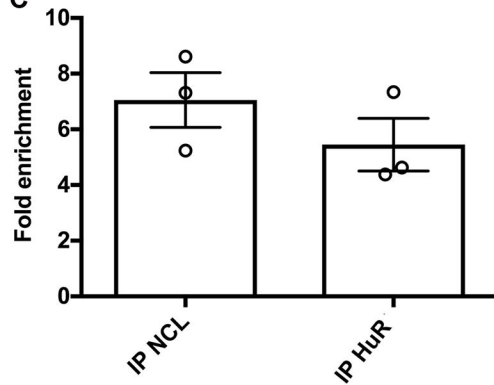
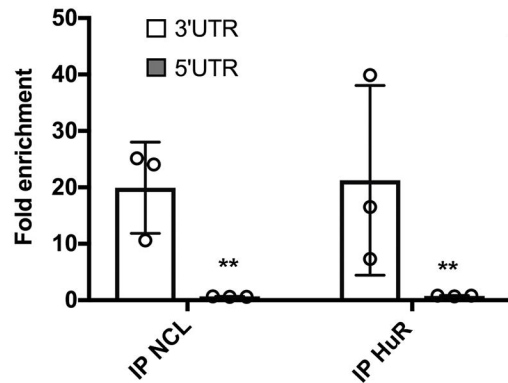
811 **Table S1:** List of primers used in this study

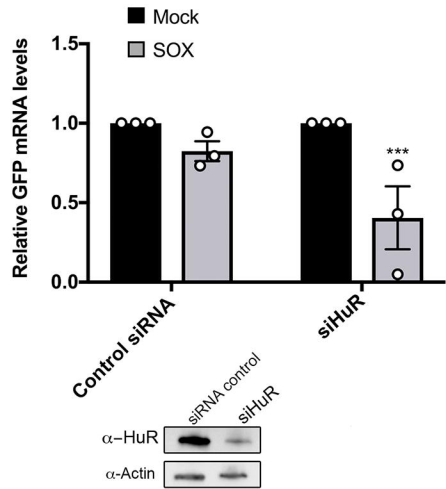
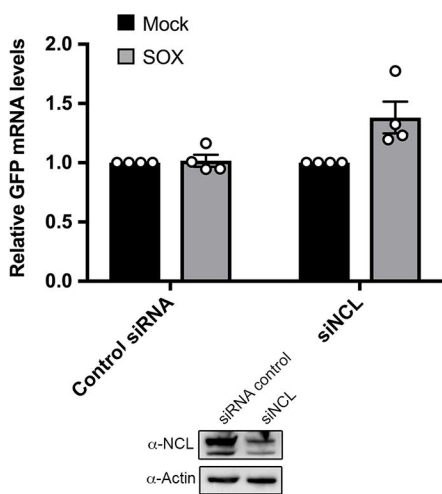


A**B****C****D**





A**B****C****D**

A**B****C**